# New Theory of Flight

Johan Hoffman[1], Johan Jansson[2] and Claes Johnson[3]
*School of Computer Science and Communication, KTH, Stockholm, Sweden*

**We present a new mathematical theory explaining the fluid mechanics of subsonic flight, which is fundamentally different from the existing circulation theory by Kutta-Zhukovsky-Prandtl formed 100 year ago. The new theory is based on a new resolution of d'Alembert's paradox showing that slightly viscous bluff body flow can be viewed as zero-drag/lift potential flow modified by a specific separation instability into turbulent flow with nonzero drag/lift. For a wing this separation mechanism maintains the large lift of potential flow generated at the leading edge at the price of small drag, resulting in a lift to drag quotient in the range $10 - 70$ which allows flight at affordable power. The new mathematical theory is supported by computed turbulent solutions of the Navier-Stokes equations with small skin friction boundary conditions in close accordance with experimental observations.**

**Nomenclature**

*L* = lift force (N)

*D* = drag force (N)

*Re* = Reynolds number (dimensionless)

$\alpha$ = angle of attack (degrees)

## I. Introduction

### A. No theory of lift and drag

The AIAA article *Quest for an Improved Explanation of Lift* by J. Hoffren from 2001 [1] states:

*"The classical explanations of lift involving potential flow, circulation and Kutta conditions are criti-*

[1] Professor, School of Computer Science and Communication, KTH, SE-10044 Stockholm, Sweden.
[2] Researcher, School of Computer Science and Communication, KTH, SE-10044 Stockholm, Sweden.
[3] Professor, School of Computer Science and Communication, KTH, SE-10044 Stockholm, Sweden.

*cized as abstract, non-physical and difficult to comprehend. The basic physical principles tend to be buried and replaced by mystical jargon."*

*"Classical explanations for the generation of lift do not make the essence of the subject clear, relying heavily on cryptical terminology and theorems from mathematics. Many classical texts even appear to have a fundamental error in their underlying assumptions."*

*"Although the subject of lift is old, it is felt that a satisfactory general but easily understandable explanation for the phenomenon (of lift), is still lacking, and consequently there is a genuine need for one."*

This remarkable state of affairs is also addressed in the New York Times article *What Does Keep Them Up There?* by Chang from 2003 [2]:

*"To those who fear flying, it is probably disconcerting that physicists and aeronautical engineers still passionately debate the fundamental issue underlying this endeavor: what keeps planes in the air?"*

NASA Glenn Research Center confirms on its web site by dismissing common explanations for lift as being incorrect, without claiming any theory to be correct. These are just a few examples of abundant evidence that there is no convincing explanation of why it is possible to fly, and that such a theory is needed.

The critical questions concern in particular the theory of flight propagated in standard textbooks [3–10] and university education, which is Kutta-Zhukovsky's circulation theory for lift illustrated in Fig. 1 and Prandtl's boundary layer theory for drag, both developed in the beginning of the last century shortly after powered flight was shown to be possible by the Wright brothers in 1903.

Before Kutta-Zhukovsky-Prandtl only Newton's impact theory [11], based on deviation of air particles by the lower side of the wing, was available, and Newton's theory showed that flight was impossible because the lift was way too small. The impossibility got further support by d'Alembert's paradox of zero lift/drag of *potential flow* as stationary irrotational incompressible flow. The observed flight of birds was thus shown impossible by mathematics, which gave theoretical fluid mechanics a bad start with effects into our time.

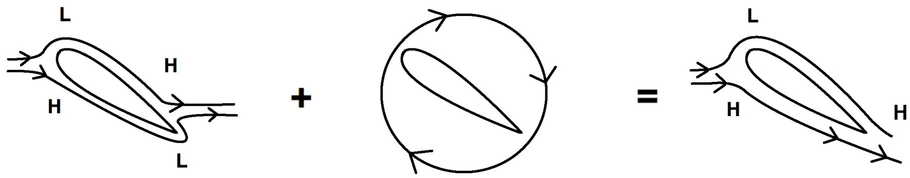


**Fig. 1 Lift by circulation according to Kutta-Zhukovsky: Potential flow with zero lift/drag resulting from high pressure at flow separation on the upper wing surface before the trailing edge of the wing (left), being modified by large scale circulation (middle) into a KZ-solution (right) with the high pressure shifted to the trailing edge thus changing the direction of the flow downwards after separation (downwash) and thereby creating lift by Newton's 3rd Law. High (H) and low (L) surface pressure is indicated in the figure.**

### B. New theory of lift and drag

In this article we present a new theory of flight supported by solid mathematics, fundamental fluid dynamics, advanced computation and substantial experimental observation, explaining the basic mechanism of the generation of lift and drag of a wing in subsonic flight.

The new theory of flight comes out from the new resolution of d'Alembert's Paradox [12] explaining that zero lift/drag potential flow cannot be observed because potential flow is unstable at separation. In the new theory the flow of air around a wing can be described as potential flow modified by a specific non-potential separation mechanism in the form of *3d rotational slip separation with point stagnation*, which reflects the basic instability of *2d irrotational potential flow separation* and gives rise to both lift and drag by avoiding the high pressure buildup of potential flow at separation on the upper surface of the wing before the trailing edge. The new theory is thus fundamentally different from the classical explanation of lift from circulation by Kutta-Zhukovsky, and the classical explanation of drag from viscosity effects by Prandtl.

Kutta-Zhukovsky obtained lift by modifying zero lift/drag potential flow by a large scale circulation around the wing section, but could not explain how that large scale circulation was generated. In the new theory unstable potential flow is instead modified into lifting flow by 3d rotational slip separation with point stagnation, which emerges as the basic physical mechanism at separation. Prandtl suggested that drag results from viscous boundary layer effects, while in the new theory drag also results from 3d rotational slip separation without boundary layers.

Experimental evidence [36] show that the classical explanation of lift from circulation by Kutta-

Zhukovsky is incorrect, since there is no high pressure buildup at separation, and the classical explanation of drag from viscosity effects by Prandtl is also incorrect, since the lack of high pressure at separation gives a significant contribution to the total drag. But the classical theory is deeply rooted as expressed in e.g. *The Origins of Lift* [13]: *"Without viscosity there would be no lift; birds and aircraft would not fly, and sailboats would not sail"*.

### C. Basic questions of a theory of flight

The basic objective of a theory of flight is to explain in mathematical terms how the flow of air around a wing can generate large *lift* $L$ (balancing gravitation) at small *drag* $D$ (requiring forward thrust) with a *lift to drag ratio* also referred to as *finesse* $\frac{L}{D}$ ranging from 10 for short wings to 70 for the long thin wings of extreme gliders, which allows flying at affordable power for both birds and airplanes? An albatross with finesse $\frac{L}{D} = 50$ can glide 50 meters upon losing 1 meter in altitude. A $525\,ton$ Airbus 380 with $\frac{L}{D} = 15$ is carried by a thrust of 35 tons, corresponding to $\frac{1}{4}$ of maximal thrust with $\frac{3}{4}$ required for accelleration at take-off. The dream of human-powered flight came true in 1977 on $60\,m^2$ wings of the *Gossamer Albatross* generating a lift of $100\,kp$ at a thrust of $5\,kp$ (thus with $\frac{L}{D} = 20$) at a speed of $5\,m/s$ supplied by a $0.3\,hp$ human powered pedal propeller.

The basic case is *subsonic flight* with the flow of air being nearly incompressible. Experience shows that subsonic flight with $\frac{L}{D} > 10$ is possible if the *Reynolds number* is larger than about $Re = 5 \times 10^5$ [14], which includes larger birds, propeller airplanes and jetliners at takeoff and landing, but not small birds and insects because the Reynolds number is too small, and not cruising jetliners in transonic flight or supersonic flight. Experience shows that $L$ increases roughly quadratically with the speed and linearly with the *angle of attack*, that is the tilting of the wing from the direction of flight, until *stall* at about 15 degrees, when $D$ abruptly increases and $L/D$ drops below 5 making sustained flight impractical.

The outline of this article is the following: in Section II we present our basic model for subsonic flight in the form of the incompressible Navier-Stokes equations, and in Section III we present the main points of the new flight theory, with in particular the role of the trailing edge of an airfoil discussed in Section IV and Section V. The classical theory is criticized in Section VI. Computational simulations of the flow past an airfoil at different angles of attack are analyzed in Section VII, and the basic mechanism of 3d rotational slip separation is analyzed in Section VIII. We give a brief summary of the article in Section IX.

## II. Basic model

Our basic model of subsonic flight is the *incompressible Navier-Stokes equations* with small viscosity. We compute solutions using a slip boundary condition as a model of the small skin friction of slightly viscous flow and obtain turbulent solutions which are validated against experiments. With less than one million mesh points we can compute solutions in close agreement with experiments, since with slip boundary conditions we do not need to resolve the thin boundary layers arising from no-slip boundary conditions, which if attempted would require impossible trillions of mesh points [15].

The Navier-Stokes equations for an incompressible fluid of unit density with small viscosity $\nu > 0$ and small skin friction $\beta \geq 0$ filling a volume $\Omega$ in $\mathbf{R}^3$ surrounding a solid body with boundary $\Gamma$ over a time interval $I = [0, T]$, take the following form: Find the velocity $u = (u_1, u_2, u_3)$ and pressure $p$ depending on $(x, t) \in \Omega \cup \Gamma \times I$, such that

$$\begin{aligned} \dot{u} + (u \cdot \nabla)u + \nabla p - \nabla \cdot \sigma &= f && \text{in } \Omega \times I, \\ \nabla \cdot u &= 0 && \text{in } \Omega \times I, \\ u_n &= g && \text{on } \Gamma \times I, \\ \sigma_s &= \beta u_s && \text{on } \Gamma \times I, \\ u(\cdot, 0) &= u^0 && \text{in } \Omega, \end{aligned} \tag{1}$$

where $\dot{u} = \frac{\partial u}{\partial t}$, $u_n$ is the fluid velocity normal to $\Gamma$, $u_s$ is the tangential velocity, $\sigma = 2\nu\epsilon(u)$ is the stress with $\epsilon(u)$ the usual velocity strain, $\sigma_s$ is the tangential stress, $f$ is a given volume force, $g$ is a given inflow/outflow velocity with $g = 0$ on a non-penetrable boundary, and $u^0$ is a given initial condition. We notice the skin friction boundary condition takes the form of a Navier-slip condition [16], coupling the tangential stress $\sigma_s$ to the tangential velocity $u_s$ with $\beta = \frac{U}{2}c_f$, where $c_f = \frac{2\sigma_s}{U^2}$ is the *skin friction coefficient*, with $\beta = 0$ for free slip (and $\beta >> 1$ for no-slip).

We observe that potential flow as stationary irrotational incompressible flow, satisfies the Navier-Stokes equations with a free slip boundary condition and vanishingly small viscosity, that is the Euler equations. We will discover that solutions of the Navier-Stokes equations with small viscosity and skin friction can be viewed as modified potential solutions, which are partly turbulent and which arise from the instability of potential flow at separation. The slip boundary condition does not give rise to boundary layers and the real flow may thus stay close to potential flow before separation.

In previous work [12, 17, 18] we show that turbulent flow can be simulated by computational solution of the Navier-Stokes equations (1) with a stabilized finite element method referred to as *G2* as an acronym for General Galerkin. G2 produces turbulent solutions characterized by substantial turbulent dissipation from the least squares stabilization of the residual acting as an automatic turbulence model, reflecting that the Navier-Stokes residual cannot be made small in turbulent regions. G2 provides automatic optimization of the computational mesh through adaptive mesh refinement based on a posteriori control of the error in chosen output functionals such as drag and lift, and we find that G2 with slip is capable of modeling slightly viscous turbulent flow with $Re > 10^5$ of relevance in many applications in aero/hydro dynamics, including flying, sailing, boating and car racing, see e.g. [19–25]. The computational cost ranges from hundred thousands of mesh points in simple geometry to millions in complex geometry.

In the framework of large eddy simulation (LES) [26], G2 can be interpreted as LES with adaptive resolution of turbulent scales based on a posteriori error estimation, and with the numerical stabilization acting as an implicit subgrid model. The slip boundary condition takes the form of a wall shear stress model of similar type as the Schumann model [27, 28]. In particular, we show that for very small skin friction the flow is insensitive to the wall shear stress model, so that the boundary layer can be modeled by a free slip boundary condition [23, 24, 29].

## III. The secret of flight

Computations with G2 reveal that flow past a wing can be seen as potential flow modified by 3d rotational slip separation at the trailing edge as illustrated in Fig. 2. In Section VIII we study the crucial 3d rotational slip separation in detail, but the effect of the modification is readily understandable in qualitative terms and then reveals the secret of flight as:

1. The zero lift/drag of potential flow results from high pressure at separation at the trailing edge, which cancels both the positive lift and the positive drag from the leading edge.

2. 3d rotational slip separation at a non-sharp trailing edge which avoids building up the high pressure of potential flow and thus generates both lift and drag.

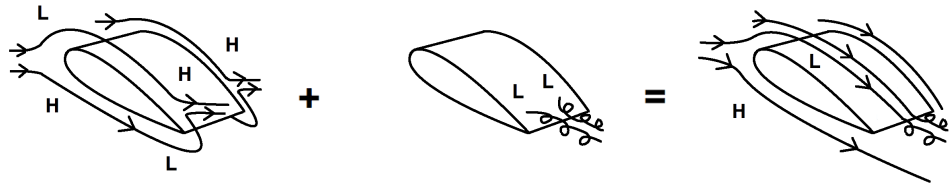


**Fig. 2 New theory showing potential flow (left) being modified at separation by the main instability mode consisting of counter-rotating rolls of streamwise vorticity attaching to the trailing edge (middle) to avoid the high pressure buildup at separation which results in a flow with downwash and lift and also drag (right), where high (H) and low (L) surface pressure is indicated in the figure.**

3. 2d potential flow can only separate at stagnation with zero flow velocity, because a solid boundary is a streamline.

4. Lift results from preservation of potential flow without separation until 3d rotational slip separation causing redirection of the flow in downwash by a combination of suction from the upper side and push from the lower side of the wing.

5. Rotational slip separation is generated by the basic instability of potential flow at separation consisting of counter-rotating low-pressure rolls of streamwise vorticity inititated as surface vorticity from meeting opposing flows, as shown in Fig. 4 and 5.

The new theory, first presented in [17, 31] with preliminary computational results, is supported by computational solutions of Navier-Stokes equations with lift and drag in close correspondence to experimental observation over the whole range of angles of attack including stall, as shown in Fig. 3 and Tables 1-4.

Also, the new theory fulfills the dream of Euler and d'Alembert as the founders of mathematical fluid mechanics of describing slightly viscous fluid flow as modified potential flow, with both potential flow and the modification amenable to analytical description, as the key to understanding of why it is possible to fly.

## IV. New theory: rounded trailing edge

The new theory has direct implications concerning the design of the trailing edge of a wing. In the classical Kutta-Zhukovsky circulation theory there is no lift without a sharp trailing edge, since lift comes from circulation supposedly determined so as to eliminate the singularity of potential flow at the sharp trailing edge. This is expressed on Wikipedia under *Kutta condition* as: *"A wing with a smoothly rounded trailing*

**Table 1 Angle of attack: $\alpha = 4°$. Tabulated values of drag and lift coefficients, from G2 computation using the software Unicorn [30] and experimental results from Ladson [35].**

| Source ($\alpha = 4°$) | $c_D$ | $c_L$ |
|---|---|---|
| Unicorn | 0.00668 $\pm 20\%$ | 0.452 $\pm 5\%$ |
| Ladson 1 | 0.00975 | 0.423 |
| Ladson 2 | 0.00823 | 0.425 |
| Ladson 3 | 0.00876 | 0.428 |

**Table 2 Angle of attack: $\alpha = 10°$. Tabulated values of drag and lift coefficients, from G2 computation using the software Unicorn [30] and experimental results from Ladson [35].**

| Source ($\alpha = 10°$) | $c_D$ | $c_L$ |
|---|---|---|
| Unicorn | 0.0144 $\pm 30\%$ | 1.11 $\pm 5\%$ |
| Ladson 1 | 0.0190 | 1.01 |
| Ladson 2 | 0.0119 | 1.05 |
| Ladson 3 | 0.0117 | 1.07 |

**Table 3 Angle of attack: $\alpha = 12°$. Tabulated values of drag and lift coefficients, from G2 computation using the software Unicorn [30] and experimental results from Ladson [35].**

| Source ($\alpha = 12°$) | $c_D$ | $c_L$ |
|---|---|---|
| Unicorn | 0.0213 $\pm 25\%$ | 1.24 $\pm 5\%$ |
| Ladson 1 | 0.0253 | 1.16 |
| Ladson 2 | 0.0132 | 1.25 |
| Ladson 3 | 0.0128 | 1.26 |

**Table 4 Post-stall. Tabulated values of drag and lift coefficients, from G2 computation using the software Unicorn [30] and experimental results from Ladson [35].**

| Source | $c_D$ | $c_L$ |
|---|---|---|
| Unicorn ($\alpha = 17°$) | 0.0790 $\pm 10\%$ | 1.09 $\pm 5\%$ |
| Unicorn ($\alpha = 20°$) | 0.230 $\pm 10\%$ | 0.998 $\pm 5\%$ |
| Ladson 1 ($\alpha = 16°$) | 0.247 | 0.893 |
| Ladson 2 ($\alpha = 18.5°$) | 0.226 | 1.06 |
| Ladson 3 ($\alpha = 18.5°$) | 0.260 | 1.19 |

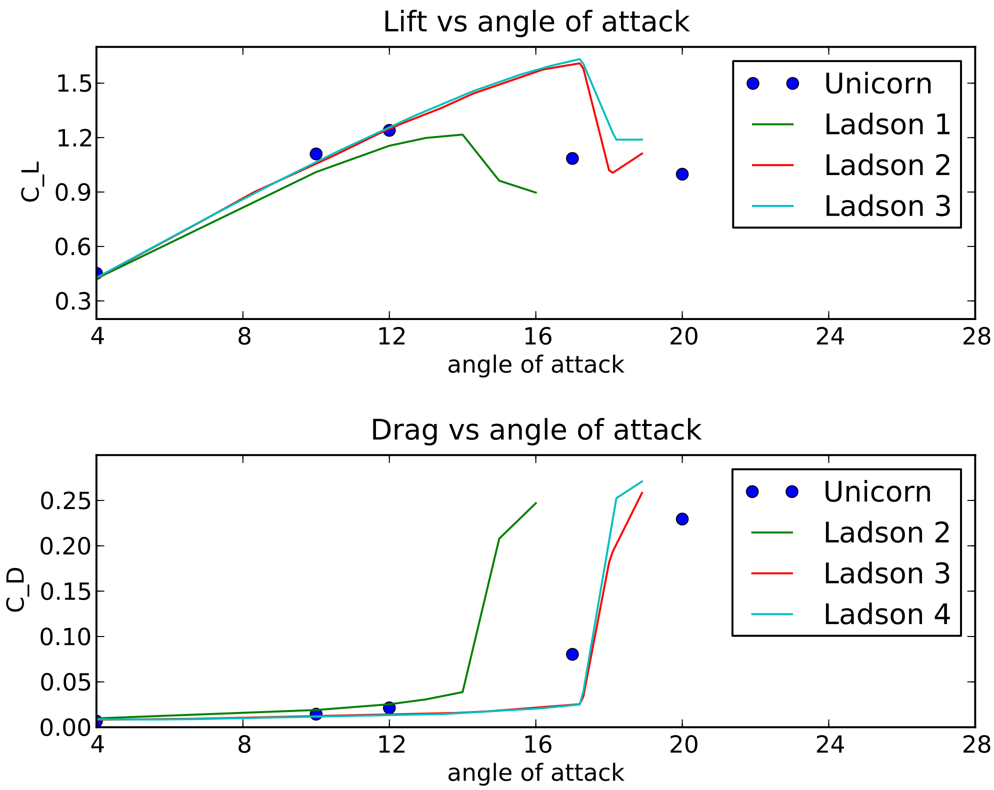


**Fig. 3 Drag and lift coefficients from G2 computation using the software Unicorn [30] plotted against the angle of attack, together with experimental results from Ladson [35].**

*edge would generate little or no lift"* or under *Airfoil* as: *"Subsonic flight airfoils have a characteristic shape with a rounded leading edge, followed by a sharp trailing edge, often with asymmetric camber"*. The UIUC Airfoil Coordinate Database [32] lists 1550 airfoils, all with sharp trailing edge.

Nevertheless, experiments were made early on [33, 34] to determine the dependence of lift and drag on the radius of the trailing edge, with the principal finding that a rounded edge of diameter less than $1\%$ of the chord length showed essentially the same lift and drag as a maximally sharp edge, while a moderate increase of drag was noted for $2\%$. The new theory assumes that the trailing edge is more or less smoothly rounded, which opens to both mathematical analysis and computation, and also fits with practice: in general real wings do not have knife-sharp trailing edges. It follows that neither practice nor theory asks for a sharp trailing edge which also makes accurate computation possible with resolution of the crucial 3d rotational slip separation pattern without excessive number of mesh points.

Observe that the idea of a sharp trailing edge, which is viewed to be essential in the Kutta-Zhukovsky circulation theory, is cumbersome both from practical point of view, because a real wing does not have a sharp trailing edge, and from mathematical point of view, because the flow has a singularity which cannot be resolved and thus analyzed and understood. The reason that the secret of flight has remained hidden for so long, can be traced to Kutta-Zhukovsky claiming that lift results from a sharp edge with a singularity and to Prandtl claiming that drag results from a vanishingly thin boundary layer, both cases being hidden from inspection: seeking physics in evasive mathematical singularities.

## V. Lift and drag invariance from scale invariance

We observe that the stationary Navier-Stokes equations with slip and vanishingly small viscosity are scale invariant in the sense that a change of the scale in space leaves the equations invariant. We therefore expect the 3d rotational separation pattern at the trailing edge to remain the same as the radius $r$ of the trailing edge tends to zero. The vorticity and pressure gradient then scales as $\frac{1}{r}$ locally, the pressure locally as $1$ with a total effect scaling as $r$, thus tending to zero with $r$. With 3d rotational separation the flow manages to separate without the high pressure of 2d potential flow, which can be seen as the secret of flight.

As the radius tends to zero the flow may be viewed to form a type of "vortex sheet" with a complex pattern of counter rotating streamwise vorticity, corresponding to oscillating high and low pressures which is small in mean by cancellation. By scale similarity we thus expect lift and drag to remain the same as the radius of the trailing edge decreases to zero, which is also observed experimentally [33, 34], as long as the Reynolds number is large enough.

For a blunt trailing edge the geometry leads to separation into an attached low pressure wake of the same size as the diameter (height) of the blunt trailing edge. As the diameter of the blunt trailing edge vanishes, again the buildup of high pressure as in potential flow is avoided.

## VI. The KZ-solution is unphysical

The KZ-solution as the potential solution modified by large scale circulation maintains the high pressure at the trailing edge of the potential solution which results in zero drag. The KZ solution is unphysical in several essential respects: A mechanism for generation of large scale circulation is missing, and the high pressure at the trailing edge of the KZ-solution giving zero drag is not seen in experiments, nor in computational simulation based on the Navier-Stokes equations.

The KZ solution was introduced as a "mathematical trick" generating lift, and has never been shown to represent the true physics. It has survived only because a convincing physical explanation has been missing. On the other hand, the new theory builds on a basic physical mechanism which can be observed in experiments, and thus the KZ solution has no longer any role to play.

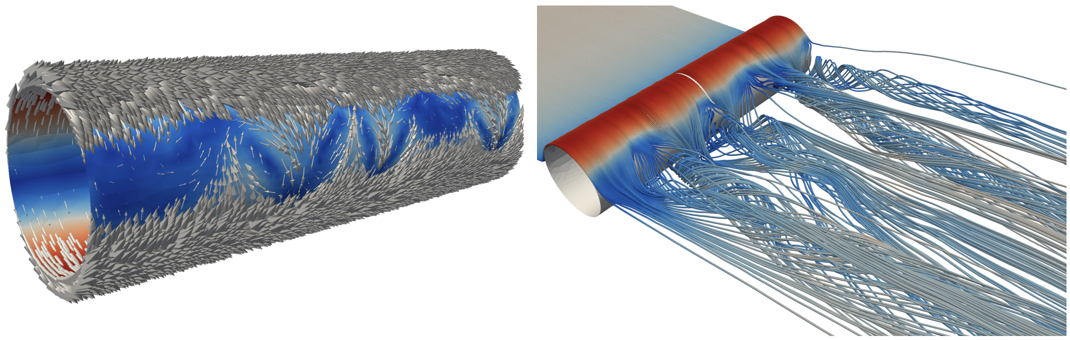

Fig. 4 Turbulent separation by surface vorticity forming counter-rotating low-pressure rolls in flow around a circular cylinder, illustrating separation at the trailing edge of a circular cylinder [29], illustrated by surface velocity (left) and streamlines (right) at a snapshot in time.

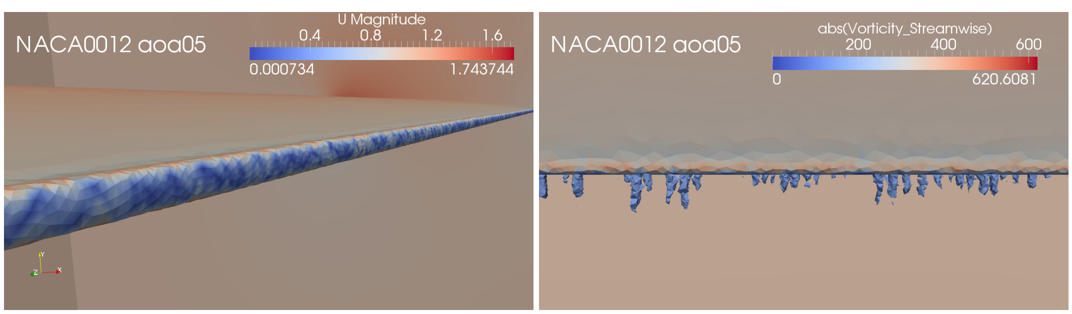


Fig. 5 Trailing edge low-pressure slip-separation at angle of attack $\alpha = 5$ for a NACA 0012 wing [23], illustrated by surface velocity magnitude (left) and vorticity magnitude in the streamwise direction (right).

## VII. Computational simulation of flight

### A. NACA 0012 wing

We support the new theory by G2 computations for a long NACA 0012 wing with lift/drag displayed in Fig. 3, and force distributions in Fig. 6-7, both in close agreement with measurement [35, 36] with $L/D \approx 30 - 50$ until beginning stall at angle of attack $\alpha \approx 14$. We summarize the findings from the computational results displayed in Fig. 6-7 with details in [23, 31], as follows :

1. *Phase 1:* $0 \leq \alpha \leq 8$

At zero angle of attack with zero lift there is high pressure at the leading edge and equal low pressures on the upper and lower crests of the wing because the flow is essentially potential and thus satisfies Bernouilli's law of high/low pressure where velocity is low/high. The drag is about 0.01 and results from rotational slip separation with low-pressure streamwise vorticity attached to the trailing edge. As $\alpha$ increases the low pressure below gets depleted as the incoming flow becomes parallel to the lower surface at the trailing edge for $\alpha = 6$, while the low pressure above intensifies and moves towards the leading edge. The streamwise vortices of the slip-separation at the trailing edge essentially stay constant in strength. The high pressure at the leading edge moves somewhat down, but contributes little to lift. Drag increases only slowly because of negative drag at the leading edge (known as leading edge suction).

Comparing our solution to the KZ-solution we find that our solution does not have the unphysical pressure rise at the trailing edge giving the KZ-solution zero drag.

2. *Phase 2:* $8 \leq \alpha \leq 14$

The low pressure on top of the leading edge intensifies as the normal pressure gradient preventing separation increases, thus creating lift peaking on top of the leading edge. The high pressure at the leading edge moves further down and the pressure below the wing increases slowly, contributing to the main lift coming from suction above. The net drag from the wing is small because of the negative drag at the leading edge (leading edge suction), with mild linear growth with respect to increasing angles of attack due to intensification and rearrangement of the pressure distribution near the leading edge. This explains why the line to a flying kite can be almost vertical even in strong wind.

3. *Phase 3:* $14 \leq \alpha \leq 16$

Beginning stall where the attached streamwise vorticity moves upstream on the upper wing surface, corresponding to near constant lift and quickly increasing drag, after which the wing essentially behaves as a bluff body with small $\frac{L}{D} \approx 1$.

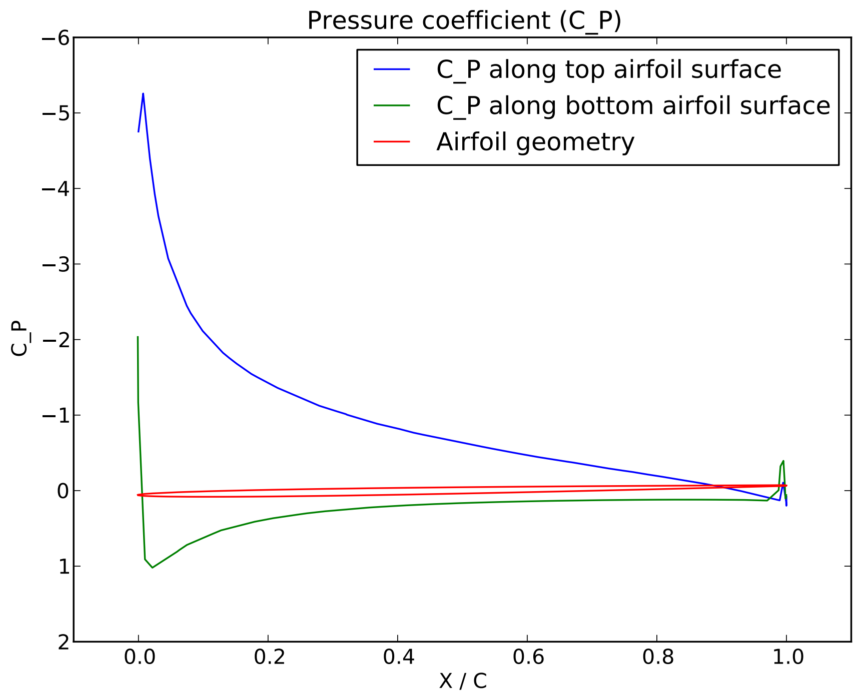


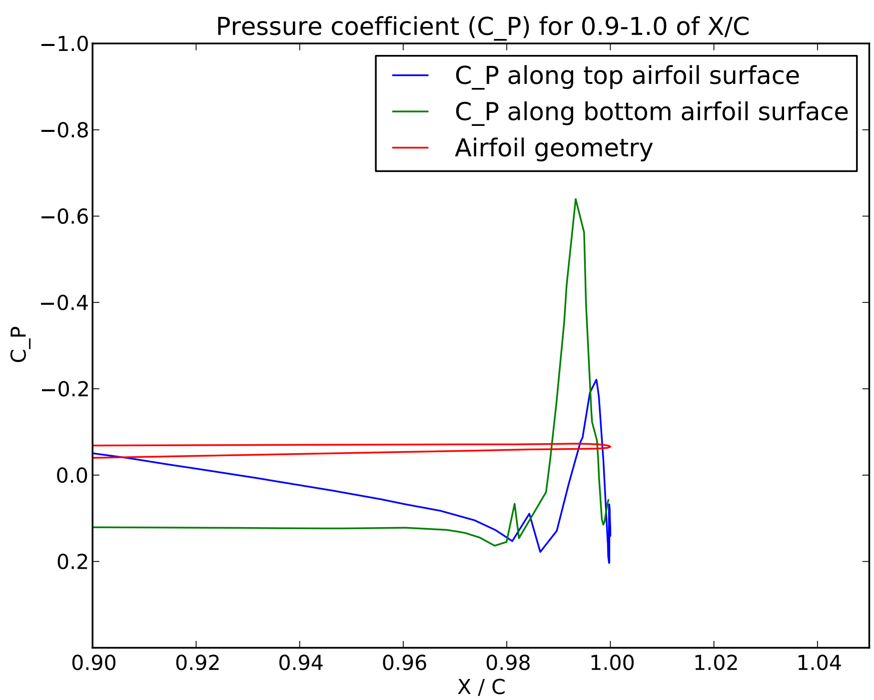


**Fig. 6 G2 computation of pressure coefficient normalized along the lower and upper parts of the wing (upper) for angle of attack 10°, averaged in time and in the spanwise direction, and a detailed view near the trailing edge of the wing. Note in particular the low pressures near rear of the wing corresponding to suction from the attached flow over the rounded trailing edge. See [23] for further details on the computations.**

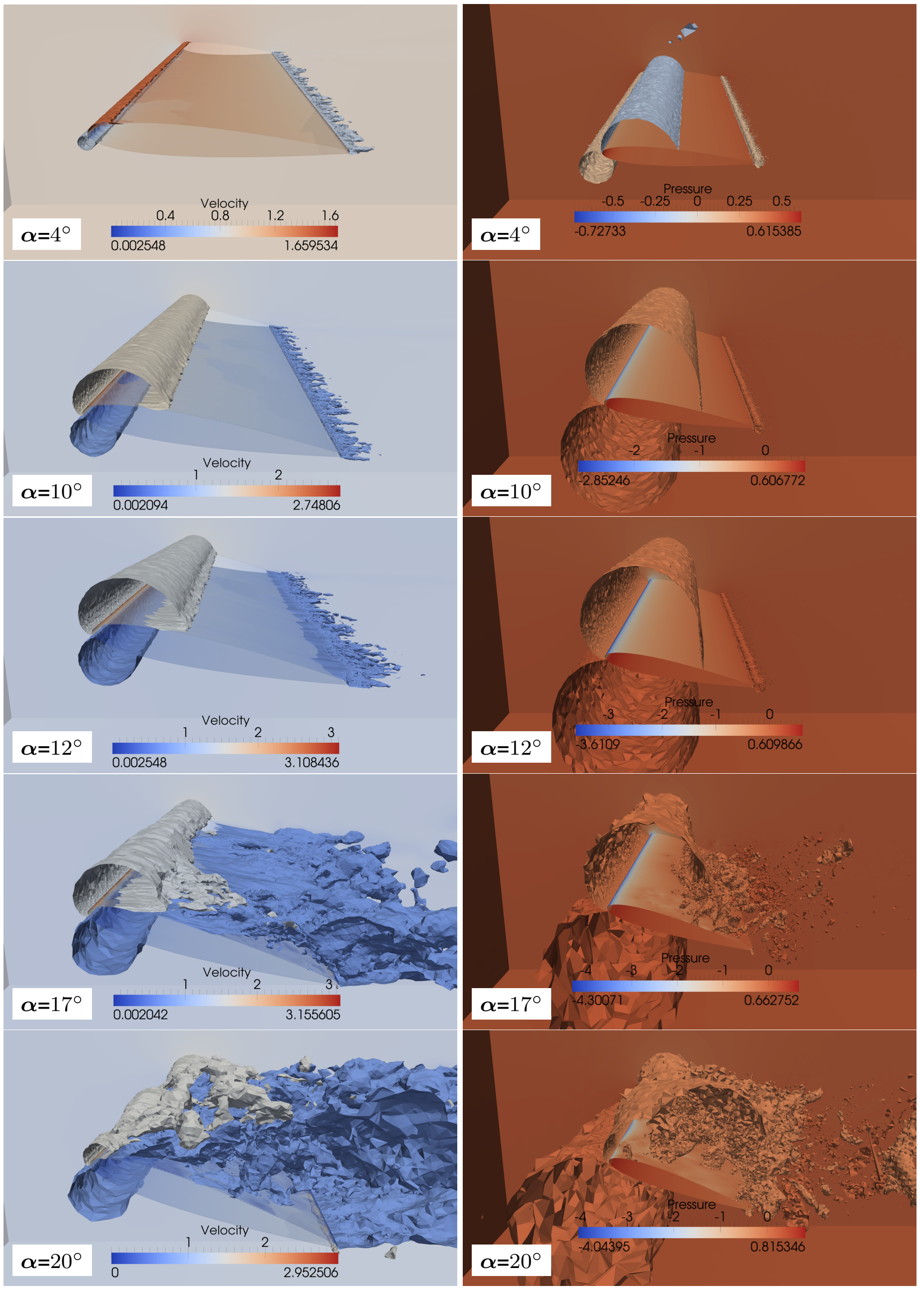


**Fig. 7 Magnitude of the velocity on the surface of the wing together with isosurfaces (left), and surface pressure with isosurfaces (right). See [23] for further details on the computations.**

## VIII. 3d rotational slip separation

### A. From unstable to quasi-stable separation

We now focus on the crucial phenomena of attachment and separation of the flow past a wing, where in particular we study the 3d stability of the flow near the trailing edge. The flow of air around a wing attaches at the leading edge and separates at the trailing edge as particles approach and leave a proximity of the wing.

Both attachment and separation require stagnation to zero flow velocity by an *adverse pressure gradient*, from opposing flows at separation and from the wing surface in attachment, which we will see makes a difference. The need of an improved analysis of 3d separation is expressed by Délery [37]:

> *"The passage from the familiar 2d to the mysterious 3d requires a complete reconsideration of concepts apparently obvious (separation and reattachment points, separated bubble, recirculation zone) but inappropriate and even dangerous to use in 3d flows."*

A linearized stability analysis is used to show that irrotational potential flow separation has an exponentially unstable mode from retarding flow with a large adverse pressure gradient, which changes the flow into *quasi-stable* 3d rotational separation with a small adverse pressure gradient and streamwise retardation, with quasi-stable signifying turbulent flow with permanent macroscopic features. The instability develops a pattern of counter-rotating low pressure tubes of streamwise vorticity attaching to the body in a zig-zag pattern around stagnation points spaced as widely as possible as illustrated in Fig. 8 for a circular cylinder. This scenario of 3d separation is supported by experiment [14, 38–41] and computer simulation [23, 24, 29], and the topology of surface patterns resulting from 3d separation has been studied for a long time [37, 42, 43]. A similar quasi-stable swirling flow can also be seen in a bathtub drain with transversal acceleration replacing the unstable retardation of fully radial flow.

## B. Stability analysis by linearization

### *1. The linearized Euler equations*

To analyze separation from a wing we study the stability of smooth solutions of the Navier-Stokes equations (1) with vanishing viscosity and skin friction, in the form of the linearized Euler equations

$$\begin{aligned} \dot{v} + (u\cdot\nabla)v + (v\cdot\nabla)\bar{u} + \nabla q &= f - \bar{f} && \text{in } \Omega\times I, \\ \nabla\cdot v &= 0 && \text{in } \Omega\times I, \\ v\cdot n &= g - \bar{g} && \text{on } \Gamma\times I, \\ v(\cdot,0) &= u^0 - \bar{u}^0 && \text{in } \Omega, \end{aligned} \tag{2}$$

where $(u,p)$ and $(\bar{u},\bar{p})$ are two Euler solutions with slightly different data, and $(v,q)\equiv(u-\bar{u},p-\bar{p})$. Formally, with $u$ and $\bar{u}$ given, this is a linear convection-reaction problem for $(v,q)$ with growth properties governed by the reaction term given by the $3\times 3$ matrix $\nabla\bar{u}$. By the incompressiblity, the trace of $\nabla\bar{u}$ is zero,

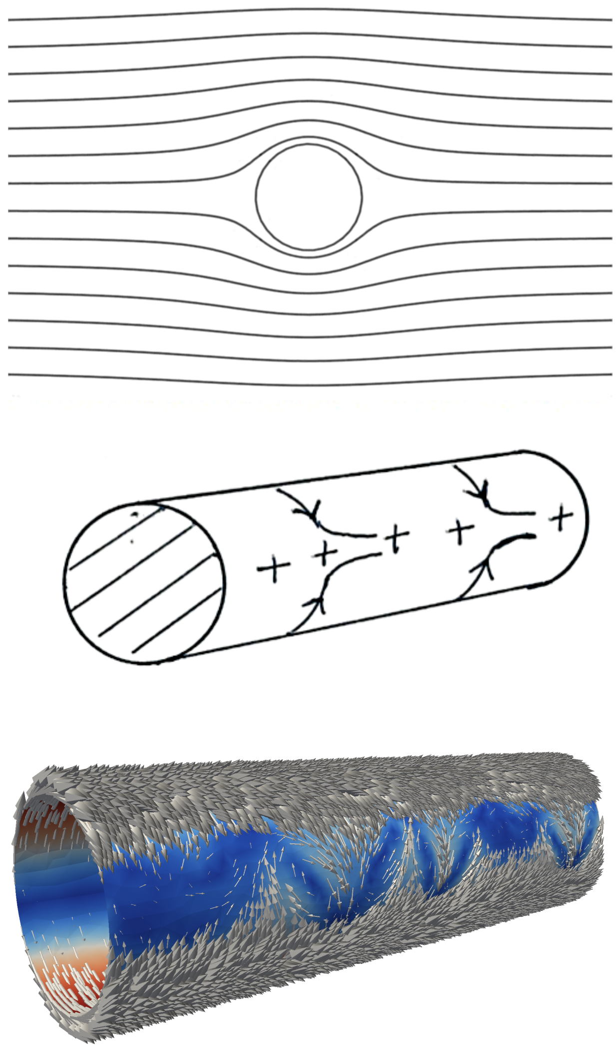

**Fig. 8 Unstable irrotational separation of potential flow around a circular cylinder (upper) form a stagnation line surrounded by a high pressure zone indicated by $+$ (middle), with corresponding opposing flow instability from a computer simulation [29] visualized by velocity glyphs and a colormap for the magnitude of the velocity (lower).**

which shows that in general $\nabla \bar{u}$ has eigenvalues with real values of both signs, of the size of $|\nabla u|$ (with $|\cdot|$ some matrix norm), thus with at least one exponentially unstable eigenvalue, except in the neutrally stable case with purely imaginary eigenvalues, or in the non-normal case of degenerate eigenvalues representing parallel shear flow [17].

The linearized equations in velocity-pressure indicate that, as an effect of the reaction term $(v \cdot \nabla)\bar{u}$:

- streamwise retardation is exponentially unstable in velocity,
- transversal acceleration is neutrally stable,

where transversal signifies a direction orthogonal to the flow direction.

Additional stability information is obtained by applying the curl operator $\nabla\times$ to the momentum equation to give the vorticity equation

$$\dot{\omega} + (u\cdot\nabla)\omega - (\omega\cdot\nabla)u = \nabla\times f \quad \text{in } \Omega, \tag{3}$$

which is also a convection-reaction equation in the vorticity $\omega = \nabla\times u$ with coefficients depending on $u$, of the same form as the linearized equations (2), with a sign change of the reaction term. The vorticity is thus also locally subject to exponential growth with exponent $|\nabla u|$:

- streamwise acceleration is exponentially unstable in streamwise vorticity (vortex stretching).

We sum up as follows: The linearized equations (2) and (3) indicate exponential growth of perturbations of velocity in streamwise retardation and of streamwise vorticity in streamwise acceleration. We shall see in more detail below that 3d rotational separation results from exponential instability of potential flow in retardation followed by vortex stretching in acceleration, with the retardation of potential flow being replaced by neutrally stable transversal acceleration.

Note that in classical analysis it is often argued that from the vorticity equation (3), it follows that vorticity cannot be generated starting from potential flow with zero vorticity and $f = 0$, which is *Kelvin's theorem*. But this is an incorrect conclusion, since perturbations $\bar{f}$ of $f$ with $\nabla\times\bar{f}\neq 0$ must be taken into account, even if $f = 0$, since general perturbations cannot be assumed to satisfy $\nabla\times\bar{f} = 0$. What you effectively see in computations is local exponential growth of vorticity on the body surface in rear retardation and by vortex stretching in acceleration, even if $f = 0$, which is a main route of instability to turbulence as well as separation.

### 2. *Exponential instability of 2d irrotational separation*

We now analyze in detail the stability of 2d irrotational separation of potential flow in a half-plane as a model of trailing edge separation: $u(x) = (x_1, -x_2, 0)$ in the half-plane $\{x_1 > 0\}$ with stagnation along the line $(0, 0, x_3)$ and

$$\frac{\partial u_1}{\partial x_1} = 1 \quad \text{and} \quad \frac{\partial u_2}{\partial x_2} = -1, \tag{4}$$

expressing that the fluid is *squeezed* by *retardation* in the $x_2$-direction and *acceleration* in the $x_1$-direction. We first focus on the retardation with the main stability feature of (2) captured in the following simplified version of the $v_2$-equation of (2), assuming $x_1$ and $x_2$ are small,

$$\dot{v}_2 - v_2 = f_2,$$

where we assume $f_2 = f_2(x_3)$ to be an oscillating perturbation depending on $x_3$ of a certain wave length $\delta$ and amplitude $h$, for example $f_2(x_3) = h\sin(2\pi x_3/\delta)$, expecting the amplitude to decrease with the wave length. We find, assuming $v_2(0,x) = 0$, that

$$v_2(t, x_3) = (\exp(t) - 1)f_2(x_3).$$

We next turn to the accelleration and then focus on the $\omega_1$-vorticity equation, for $x_2$ small and $x_1 \geq \bar{x}_1 > 0$ with $\bar{x}_1$ small, approximated by

$$\dot{\omega}_1 + x_1\frac{\partial \omega_1}{\partial x_1} - \omega_1 = 0,$$

with the "inflow boundary condition"

$$\omega_1(\bar{x}_1, x_2, x_3) = \frac{\partial v_2}{\partial x_3} = (\exp(t) - 1)\frac{\partial f_2}{\partial x_3}.$$

The equation for $\omega_1$ thus exhibits exponential growth, which is combined with exponential growth of the "inflow condition". We can see these features in principle and in computational simulation in Fig. 9 showing how opposing flows at separation generate a pattern of alternating surface vortices from pushes of fluid up/down, which act as initial conditions for vortex stretching into the fluid generating counter-rotating low-pressure tubes of streamwise vorticity.

The above model study can be extended to the full linearized equations linearized at $u(x) = (x_1, -x_2, 0)$:

$$\begin{aligned} Dv_1 + v_1 &= -\tfrac{\partial q}{\partial x_1}, \\ Dv_2 - v_2 &= -\tfrac{\partial q}{\partial x_2} + f_2(x_3), \\ Dv_3 &= -\tfrac{\partial q}{\partial x_3}, \\ \nabla \cdot v &= 0, \end{aligned} \tag{5}$$

where $Dv = \dot{v} + u \cdot \nabla v$ is the convective derivative with velocity $u$ and $f_2(x_3)$ as before. We here need to show that the force perturbation $f_2(x_3)$ will not get cancelled by the pressure term $-\frac{\partial q}{\partial x_2}$ in which case the exponential growth of $v_2$ would get cancelled. Now $f_2(x_3)$ will induce a variation of $v_2$ in the $x_3$ direction, but this variation does not upset the incompressibility since it involves the variation in $x_2$. Thus, there is no reason for the pressure $q$ to compensate for the force perturbation $f_2$ and thus exponential growth of $v_2$ is secured.

We thus discover streamwise vorticity generated by a force perturbation oscillating in the $x_3$ direction, which in the retardation of the flow in the $x_2$-direction creates exponentially increasing vorticity in the $x_1$-direction, which acts as inflow to the $\omega_1$-vorticity equation with exponential growth by vortex stretching. We find exponential growth at rear separation in both the retardation in the $x_2$-direction and the acceleration in the $x_1$-direction, as a result of the squeezing expressed by (4).

The corresponding pressure perturbation changes the high pressure at separation of potential flow into a zig-zag alternating more quasi-stable pattern of moderate pressure variations with elevated pressure zones deviating opposing flow into non-opposing streaks which are captured by low pressure zones to form rolls of streamwise vorticity allowing the flow to spiral away from the body. This is similar to the vortex formed in a bathtub drain.

The larger the scale of the vortices, the more stable is the rotational separation, since unstable streamwise retardation can be minimized. The most stable configuration of the zig-zag pattern of vortices is thus the one corresponding to the maximal size of the vortices allowed by the geometry with minimal retardation. At start-up from zero velocity, streamwise vorticity is triggered from perturbation on the same scale as the mesh size, which is rapidly modified into mesh independent large scale streamwise vortices given by the scale of the geometry. We shall see that the tubes of low-pressure streamwise vorticity change the normal pressure gradient to allow separation without unstable retardation, but the price is generation of drag by elimination of the high pressure of zero drag potential flow as a “cost of separation”.

### *3. Neutrally stable transversal acceleration*

As a model of flow with transversal acceleration we consider the potential velocity $u = (0, x_3, -x_2)$ of a constant rotation in the $x_1$-direction, with the corresponding linearized equations

$$\dot{v}_1 = 0, \quad \dot{v}_2 + v_3 = 0, \quad \dot{v}_3 - v_2 = 0, \tag{6}$$

which model a neutrally stable harmonic oscillator without exponential growth corresponding to imaginary eigenvalues of the matrix $\nabla u$.

#### *4. Quasi-stable potential flow attachment*

The above analysis also shows that potential flow attachment, even though it involves streamwise retardation, is quasi-stable. This is because the initial perturbation $f_2$ in the above analysis is forced to be zero by the slip boundary condition requiring the normal velocity to vanish. In short, potential flow attachment is stable because the flow is retarded by the solid body and not by opposing flows as in separation.

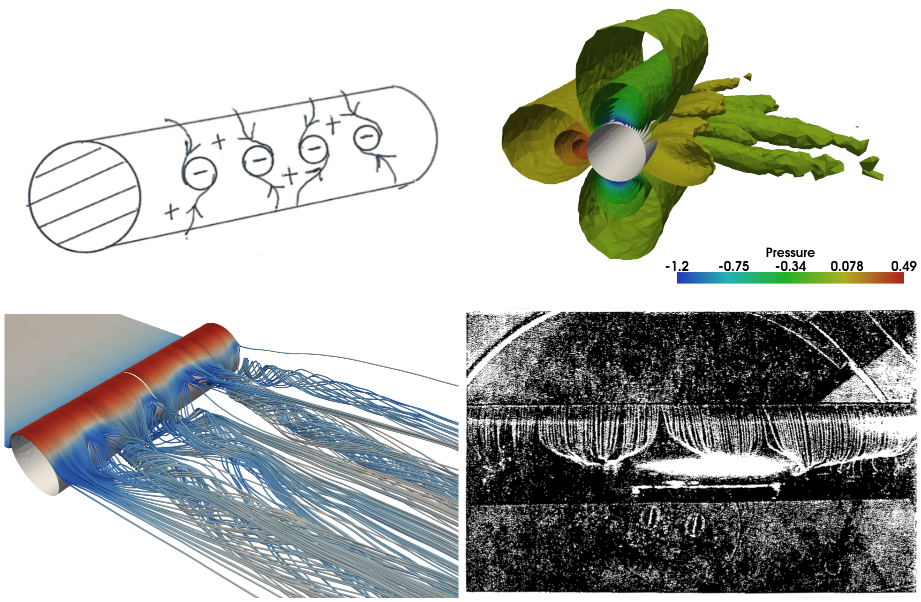


**Fig. 9 Quasi-stable 3d rotational separation for a circular cylinder from alternating high/low (+/-) pressure: principle (upper left) and computer simulation [29] (upper right), streamlines from computer simulation [29] (lower left) and silk threads in experiment [40] (lower right) .**

### C. Attachment and separation in flow past a circular cylinder

The flow around a circular cylinder can be used as a model of both leading edge attachment and rounded trailing edge separation for a wing. We thus consider the flow around a long circular cylinder, of unit radius with axis along the $x_3$-axis in $\mathbf{R}^3$ with coordinates $x = (x_1, x_2, x_3)$, assuming the flow velocity is $(1, 0, 0)$ at infinity in each $x_2x_3$-plane, which in polar coordinates $(r, \theta)$ in a plane orthogonal to the cylinder axis is given by the potential function, see Fig. 8,

$$\varphi(r,\theta) = (r + \frac{1}{r})\cos(\theta)$$

with corresponding velocity components

$$u_r \equiv \frac{\partial\varphi}{\partial r} = (1 - \frac{1}{r^2})\cos(\theta), \quad u_s \equiv \frac{1}{r}\frac{\partial\varphi}{\partial\theta} = -(1 + \frac{1}{r^2})\sin(\theta)$$

with streamlines being level lines of the conjugate potential function

$$\psi \equiv (r - \frac{1}{r})\sin(\theta).$$

Potential flow is constant in the direction of the cylinder axis with velocity $(u_r, u_s) = (1, 0)$ for $r$ large, is fully symmetric with zero drag/lift, attaches and separates at the lines of stagnation $(r, \theta) = (1, \pi)$ in the front and $(r, \theta) = (1, 0)$ in the back. By Bernouilli's principle the pressure is given by

$$p = -\frac{1}{2r^4} + \frac{1}{r^2}\cos(2\theta)$$

when normalized to vanish at infinity. We compute

$$\frac{\partial p}{\partial\theta} = -\frac{2}{r^2}\sin(2\theta), \quad \frac{\partial p}{\partial r} = \frac{2}{r^3}(\frac{1}{r^2} - \cos(2\theta)),$$

and discover an adverse pressure gradient in the back. Potential flow around a circular cylinder shows exponentially unstable 2d irrotational separation and quasi-stable 2d attachment, and is a useful model for both attachment at the leading edge of a wing and separtion at a rounded trailing edge.

The flow past a circular cylinder is well investigated experimentally for low Reynolds numbers, and studies are available also for high Reynolds number flow where boundary layers are turbulent, of relevance for the present discussion [41]. The flow past a cylinder is characterized by successive transition to turbulence in the wake, the shear layers, and finally the boundary layers (referred to as the *ultimate region* [41]). From available experimental data in the literature we note in particular two phenomena associated with transition in the boundary layers; (i) *drag crisis*, a sudden drop in drag since separation is delayed, and (ii) development of transversal structures of streamwise vorticity, also referred to as *cells*, attached to the downstream side of the cylinder of a similar size as the cylinder diameter [14, 39, 40]. The scenario of quasi-stable3d rotational 3d separation fits well with experimental observations, as an explanation of both drag crisis and streamwise vorticity cells.

Solving the Navier-Stokes equations by G2 we find that a flow initialized as potential flow develops into a turbulent solution with rotational separation as identified above, see Fig. 9. Detailed computational studies of the flow past a circular cylinder [29] show convergence in macroscopic flow features and drag force prediction with respect to mesh refinement. Large skin friction $\beta$ results in a solution where the flow is forced to satisfy a no slip condition, with $\beta$ acting as a penalty parameter. As the skin friction $\beta$ is reduced, modeling an increased Reynolds number, the drag crisis phenomenon (i) is reproduced with also development of stable streamwise vorticity structures (ii), with a validated quantitative prediction of the drag force beyond drag crisis. A sensitivity study with respect to the skin friction parameter $\beta$ also shows that macroscopic features, including the separation pattern, are insensitive to small $\beta$.

## IX. Summary

We have presented a new theory for subsonic flight which is fundamentally different from the classical theory associated to Kutta-Zhukovsky-Prandlt, with lift from potential flow modified by circulation and drag from viscous boundary layers. In the new theory lift and drag generation can be understood from a modification of potential flow by a 3d instability mechanism, resulting in 3d rotational separation with streamwise vorticity attached to the trailing edge.

The quasi-stable patterns of 3d rotational separation is identified in qualitative analytical terms as unstable retardation in irrotational potential flow replaced by neutrally stable transversal acceleration, a scenario which is supported by computational simulation and experimental observation in the literature, for a cylinder as a model of a rounded trailing edge and also for wings, and more general bluff or streamlined bodies.

The new theory opens for direct approximation of aerodynamic forces of wings and airplanes through computational solution of the incompressible Navier-Stokes equations with small skin friction boundary conditions without resolution of thin turbulent boundary layers.


## Acknowledgments

The authors would like to acknowledge the financial support provides by the European Research Council, the Swedish Foundation for Strategic Research, and the Swedish Research Council. The simulations were performed on resources provided by the Swedish National Infrastructure for Computing (SNIC) at PDC - Center for High-Performance Computing.

## References


[1] J. Hoffren, Quest for an improved explanation of lift, AIAA 2001-0872, 39th AIAA Aerospace Sciences Meeting and Exhibit, Reno, 2001.

[2] Kenneth Chang; Staying Aloft: What keeps them up there?, New York Times, Dec 9, 200

[3] Prandtl, Essentials of Fluid Mechanics, Herbert Oertel (Ed.), 2004.

[4] Introduction to the Aerodynamics of Flight, Theodore A. Talay, Langley Reserach Center, 1975.

[5] Aerodynamics of the Airpoplane, Hermann Schlichting and Erich Truckenbrodt,Mac Graw Hill, 1979.

[6] Fundamentals of Aerodynamics, John D Anderson, 2010.

[7] Aerodynamics, Aeronautics and Flight Mechanics, McCormick, 1995.

[8] Aerodynamics, Krasnov, 1978.

[9] Aerodynamics, von Karmann, 2004.

[10] Theory of Flight, Richard von Mises, 1959.

[11] J. S. Calero, The Genesis of Fluid Mechanics 1640-1780, Studies in History and Philosophical Sciense 22, Springer, 2008.

[12] J. Hoffman and C. Johnson, Resolution of d'Alembert's paradox, J. Math. Fluid Mech., Vol.12(3), pp.321-334, 2010.

[13] Arvel Gentry, The Origins of Lift, 2006.

[14] G. Schewe, Reynold's-number effects in flow around more or less bluff bodies, 4 Intern. Colloquium Bluff Body Aerodynamics and Applications, also in Journ. Wind Eng. Ind. Aerodyn. 89 (2001).

[15] J. Kim and P. Moin, Tackling Turbulence with Supercomputer, Scientific American.

[16] C.L.M.H. Navier. Memoire sur les lois du mouvement des fluides. Mem. Acad. R. Sci. Paris., 6:389ï£¡416, 1823.

[17] J. Hoffman and C. Johnson, Computational Turbulent Incompressible Flow, Springer 2007.

[18] J. Hoffman and C. Johnson, Blowup of Euler solutions, BIT Numerical Mathematics, Vol 48, No 2, 285-307.

[19] J. Hoffman, C. Johnson, A new approach to computational turbulence modeling, Comput. Methods Appl. Mech. Engrg. 195 (2006) 2865–2880.

[20] J. Hoffman, Computation of mean drag for bluff body problems using adaptive dns/les, SIAM J. Sci. Comput., 27(1) (2005), pp. 184–207.

[21] J. Hoffman, Adaptive simulation of the turbulent flow past a sphere, J. Fluid Mech., 568 (2006), pp. 77–88.

[22] J. Hoffman, Efficient computation of mean drag for the subcritical flow past a circular cylinder using general galerkin g2, Int. J. Numer. Meth. Fluids, 59(11) (2009), pp. 1241–1258.

[23] J.Jansson, J.Hoffman and N.Jansson, Simulation of 3D flow past a NACA 0012 wing section, in review (available as CTL technical report kth-ctl-4023).

[24] R. Vilela De Abreu, N. Jansson and J. Hoffman, Adaptive computation of aeroacoustic sources for rudimentary landing gear, in proceedings for Workshop on Benchmark problems for Airframe Noise Computations I, Stockholm, 2010.

[25] N. Jansson, J. Hoffman, M. Nazarov, Adaptive Simulation of Turbulent Flow Past a Full Car Model, in: Proceedings of the 2011 ACM/IEEE International Conference for High Performance Computing, Networking, Storage and Analysis, SC '11, 2011.

[26] P. Sagaut, Large Eddy Simulation for Incompressible Flows (3rd Ed.), Springer-Verlag, Berlin, Heidelberg, New York, 2005.

[27] U. Piomelli and E. Balaras, Wall-layer models for Large-eddy simulation, Annu. Rev. Fluid Mech., Vol.34, pp.349-374, 2002.

[28] U. Schumann, Subgrid scale model for finite difference simulations of turbulent flows in plane channels and annuli, J. Comput. Phys. 18 (4) (1975) 376 – 404

[29] J. Hoffman and N. Jansson, A computational study of turbulent flow separation for a circular cylinder using skin friction boundary conditions, in proceedings for Quality and Reliability of Large-Eddy Simulations II, Pisa, Italy, 2009.

[30] J. Hoffman, J. Jansson, C. Degirmenci, N. Jansson, M. Nazarov, Unicorn: A Unified Continuum Mechanics Solver, in: Automated Scientific Computing, Springer, 2012.

[31] J. Hoffman and C. Johnson, Mathematical Secret of Flight, Normat, Vol.57, pp.145-169, 2009.

[32] UIUC Airfoil Data Site, http://www.ae.illinois.edu/m-selig/ads.html

[33] J. Stack, W. F. Lindsay, NACA Technical Report 665, 1938.

[34] L. Joseph Herrig, James C. Emery and John R. Erwin, Effects of Section Thickness and Trailing-Edge Radius on TBE Performance of NAAC 65smms Compressor Blades in Cascade, NACA Research Memorandum L51J16, 1956.

[35] C. Ladson, U. S. N. Aeronautics, S. A. Scientific, T. I. Division, Effects of independent variation of Mach and Reynolds numbers on the low-speed aerodynamic characteristics of the NACA 0012 airfoil section, NASA technical memorandum, National Aeronautics and Space Administration, Scientific and Technical Information Division, 1988.

[36] N. Gregory, C. C.L. O'Reilly, Low-speed aerodynamic characteristics of NACA 0012 aerofoil section, including the effects of upper-surface roughness simulating hoar frost, Aeronautical Research Council (Great Britain), Reports and memoranda, H.M.S.O., 1973.

[37] J. M. Delery, R. Legendre and Henri Werle: Toward the elucidation of three-dimensional separation, Annu. Rev. Fluid. Mech. 2001 33:129-54.

[38] B. Gölling, Experimentelle Untersuchungen des laminar-turbulenten Ueberganges der Zylindergrenzschichtströmung, DLR, 2001.

[39] J. S. Humphreys, On a circular cylinder in a steady wind at transition Reynolds numbers, Journal of Fluid Mechanics, Vol.9(4), pp.603-612, 1960.

[40] A. I. Korotkin, The three dimensionality of the flow transverse to a circular cylinder, Fluid Mechanics - Soviet Research, Vol.5, 1976.

[41] M. M. Zdravkovich, Flow around circular cylinders: a comprehensive guide through flow phenomena, experiments, applications, mathematical models, and simulations. Vol.1 [Fundamentals], Oxford Univ. Press, Oxford, 1997.

[42] M. Tobak and D. J. Peake, Topology of three dimensional separated flow, Ann. Rev. Fluid Mech., Vol.14, pp.61-85, 1982.

[43] U. Dallmann, Three-dimensional vortex structures and vorticity topology, Fluid Dynamics Research, Vol.3, pp.183-189, 1988.